Materials Transactions, Vol. 43, No. 8 (2002) pp. 1827 to 1832
Special Issue on Lead-Free Electronics Packaging

Effects of Alloying in Near-Eutectic Tin–Silver–Copper Solder Joints

Iver E. Anderson, Bruce A. Cook, Joel Harringa, Robert L. Terpstra, James C. Foley and Ozer Unal

Ames Laboratory, Iowa State University, Ames, Iowa 50011, USA

This study included a comparison of the baseline Sn–3.5Ag eutectic to one near-eutectic ternary alloy, Sn–3.6Ag–1.0Cu and two quaternary alloys, Sn–3.6Ag–1.0Cu–0.15Co and Sn–3.6Ag–1.0Cu–0.45Co, to increase understanding of the effects of Co on Sn–Ag–Cu solder joints cooled at 1–3°C/s., typical of reflow assembly practice. The results revealed joint microstructure refinement due to Co-enhanced nucleation of the Cu_6Sn_5 phase in the solder matrix, as suggested by Auger elemental mapping and calorimetric measurements. The Co also reduced intermetallic interface faceting and improved the ability of the solder joint samples to maintain their shear strength after aging for 72 h at 150°C. Some recent additional results with Co and Fe additions are consistent with this catalysis effect, where a reduced total solute level was tested. The baseline Sn–3.5Ag joints exhibited significantly reduced strength retention and coarser microstructures.

(Received April 30, 2002; Accepted July 10, 2002)

Keywords: *lead-free solder, tin (Sn)-silver (Ag)-copper (Cu) solders, joint shear strength, joint microstructure, solder joint solidification*

1. Introduction

Environmental concerns and worldwide market forces have accelerated the development of Pb-free solders for electronic assembly with considerable effort focussed on near-eutectic Sn–Ag–Cu alloys, based on the discovery of a ternary eutectic at 217°C with Sn–4.7Ag–1.7Cu (mass%) as the proposed composition.[1,2] While many studies have demonstrated that Sn–Ag–Cu may substitute for Sn–37Pb (mass%) eutectic solder ($T_e = 183$°C) in general joining tasks, recent results have shown that these solders also provide a marked improvement over Sn–Pb in high temperature, high stress applications, even exceeding Sn–3.5Ag (mass%) eutectic solder.[3] Although Sn–Ag ($T_e = 221$°C) is a well-known alternative to Sn–Pb for high temperature applications, alloys in the Sn–Ag–Cu solder family have baseline advantages of a reduced melting temperature and an additional strengthening phase, Cu_6Sn_5.[2] When studied in comparison to many other binary, ternary, and quaternary Pb-free alloys, the broad potential of Sn–Ag–Cu solders has been recognized by several industrial groups throughout the world.[2] The European IDEALS consortium currently recommends one specific alloy, Sn–3.8Ag–0.7Cu (mass%), for Pb-free reflow applications.[4] The Pb-free roadmap of the Japan Electronic Industry Development Association (JEIDA) recommends in its "short list" the Sn–(2 to 4)Ag–(0.5 to 1)Cu (mass%) alloys both for wave applications and for reflow at "medium and high temperatures."[5] In North America, the Lead-free Assembly Project of the National Electronics Manufacturing Initiative (NEMI) has established a very specific list of Pb-free solder alloys for accelerated development, focussing on Sn–3.9Ag–0.6Cu (mass%) for reflow applications.[4]

As an ongoing fundamental research activity, our group has concentrated most recently on understanding of the composition dependence of the solder joint solidification microstructure in near-eutectic Sn–Ag–Cu and Sn–Ag–Cu–X alloys, as affected by variations in the solidification conditions.[6–8] The pursuit of understanding of the effect of Co on the as-solidified microstructure of model solder joints made with Sn–Ag–Cu–Co will be the main subject of this paper. Our initial analysis[6] revealed a significant refinement of the bulk solder joint microstructure, more refined than the effect induced by either the Fe or Ni additions. A highly refined solder bulk microstructure could significantly improve thermal-mechanical fatigue resistance, if the refinement could be retained during temperature/stress fatigue cycling.[9] A single-mode shear strength test method was used[10] to compare Sn–Ag–Cu–Co solder joint samples relative to joints made from near-eutectic Sn–3.6Ag–1.0Cu and eutectic Sn–3.5Ag. These asymmetric four-point bend (AFPB) samples were examined by SEM and shear tested in both as-solidified and aged conditions.

2. Experimental Procedure

This study included a comparison of solder joint samples made from the baseline Sn–3.5Ag (mass%) eutectic to joint samples made from one near-eutectic (NE) ternary alloy, Sn–3.6Ag–1.0Cu and two quaternary alloys, Sn–3.6Ag–1.0Cu–0.15Co and Sn–3.6Ag–1.0Cu–0.45Co. Solder joint microstructure and shear strength were examined using a model joint sample configuration, a Cu/solder/Cu butt joint. The solder joint sample was designed to permit hand soldering at 255 to 260°C with solid solder wire and a fairly aggressive water-based flux containing ZnCl and HCl (obtained from Johnson Mfg. of Princeton, IA), with a nominal joint gap of 0.076 mm. Joint cooling conditions were manipulated[8] to mimic realistic reflow conditions,[11] 1–3°C/s. The finished sample was sectioned into AFPB test bars, as shown in Fig. 1(a), to facilitate single mode shear testing, both as-solidified and after aging for 72 h at 150°C. AFPB shear tests were performed with the fixture shown in Fig. 1(b) on a screw-driven testing machine in a compressive mode at a rate of 0.1 mm/min at ambient temperature. Joint sample microstructures were examined in the as-solidified condition. Solder alloy melting and solidification behavior was measured by differential scanning calorimetry (DSC) in droplet emulsion samples[12] to assess the undercooling differences between the ternary NE alloy, Sn–3.6Ag–1.0Cu, and one Co-modified quaternary, Sn–3.6Ag–1.0Cu–0.45Co. The DSC

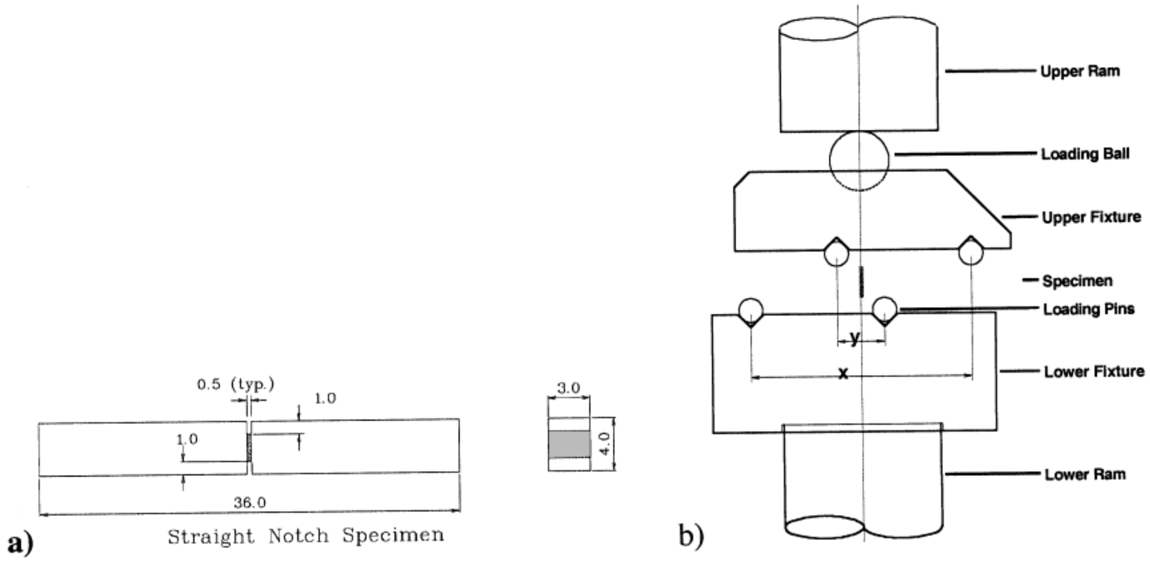

Fig. 1 Schematic showing a) the specimen geometry with dimensions in mm and b) a side view of the test fixture used in the asymmetric four-point bend tests, where x = 30 mm and y = 4 mm. Adapted from ref. 7).

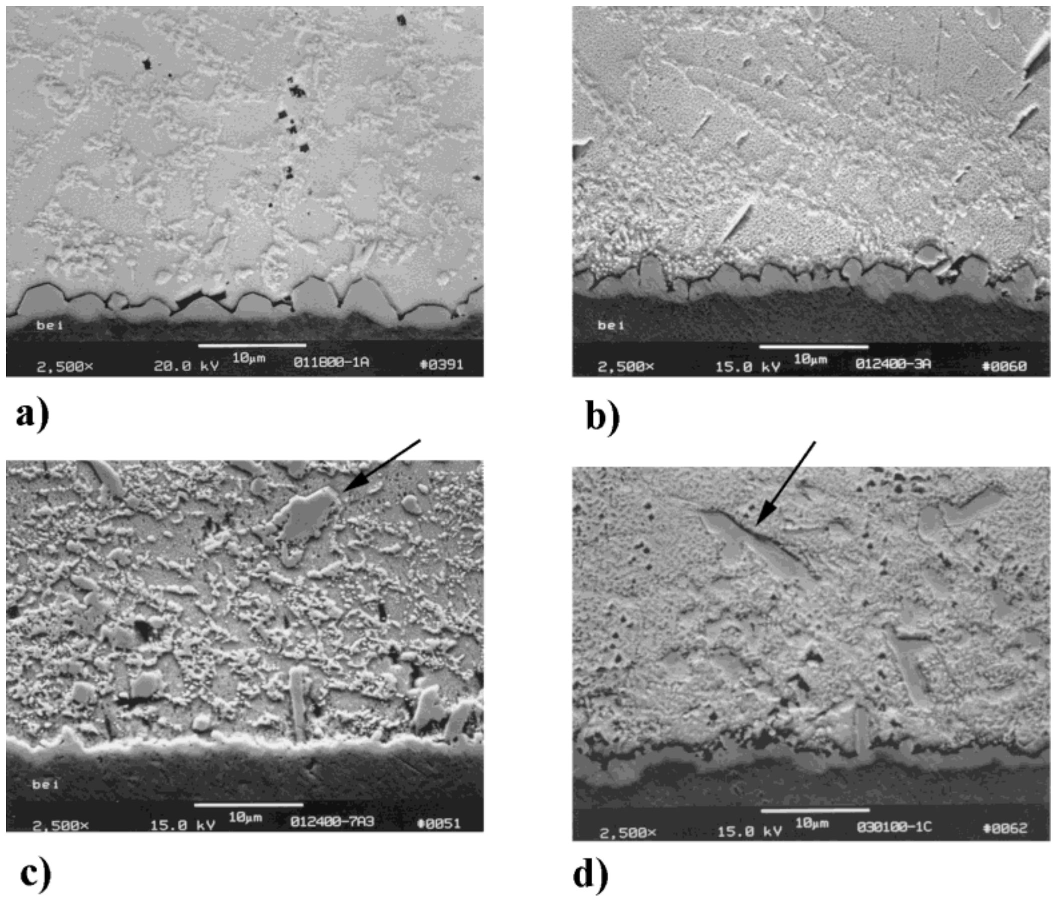

Fig. 2 SEM micrographs, using backscattered electron imaging, showing Cu substrate (bottom), intermetallic Cu/solder interface, and solder matrix microstructures at moderate magnification of slowly cooled joints. a) Sn–3.5Ag, b) Sn–3.6Ag–1.0Cu, c) Sn–3.6Ag–1.0Cu–0.15Co, and d) Sn–3.6Ag–1.0Cu–0.45Co. Arrows indicate examples of the blocky intermetallic phase in the solder matrix regions.

heating (250°C, reversal point) and cooling thermograms were measured at 40°C/min., after instrument calibration with pure Sn at the same rate. Scanning Auger electron microscopy also permitted analysis of the distribution of Co in the microstructure of a solder joint made from the Sn–3.6Ag–1.0Cu–0.45Co alloy.

3. Results

The SEM results in Fig. 2(a) through Fig. 2(d) revealed a progression in microstructural refinement of the joint matrix and the solder/substrate interface; first, from Cu modification of the Sn–Ag eutectic, which suppressed Sn den-

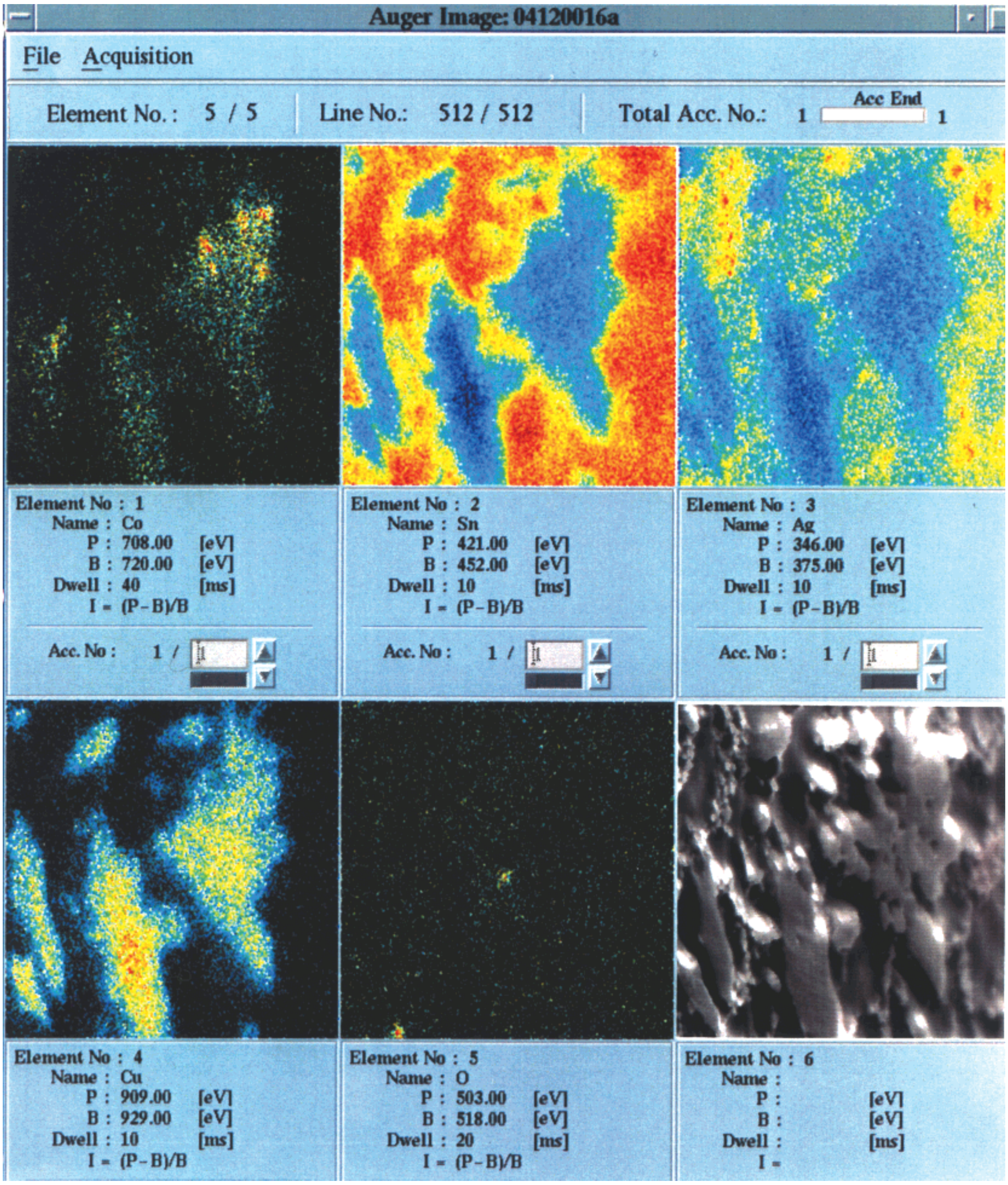

Fig. 3 Composite of Auger elemental mapping results for the solder matrix region of a joint made from Sn–3.6Ag–1.0Cu–0.45Co, where the SEM micrograph in secondary electron imaging at the lower right corner serves as the template for the elemental maps of Co, Sn, Ag, Cu, and O. Reprinted from ref. 14).

drite formation. The Co additions to the near-eutectic Sn–Ag–Cu also appeared to refine the as-solidified microstructure scale by adding additional Cu_6Sn_5 primary phase particles to the ternary eutectic mixture. In general from Figs. 2(c) and (d), the Co addition appeared to reduce intermetallic interface faceting, as evidenced by the fine scale "bumps" seen along the interface with the solder joint matrix phase. Also, the Co addition seems to enhance formation of the Cu_6Sn_5 phase in the solder matrix as a well-distributed, blocky intermetallic phase (arrows point to examples in Figs. 2(c) and (d)), compared to that in the near-eutectic phase mixture of Fig. 2(b).

One explanation for the transition in as-solidified microstructure from the addition of as little as 0.15Co could be related to the initial alloy design hypothesis[6,8,13)] that considered Co as a substitutional solute addition to the Cu_6Sn_5 phase. To investigate whether Co was not only distributed within the Cu_6Sn_5 phase as a solute, but perhaps was also concentrated in some regions as an effective nucleation catalyst for Cu_6Sn_5, a polished and lightly etched cross-section of a joint made from Sn–3.6Ag–1.0Cu–0.45Co was examined by scanning Auger electron microscopy. The elemental mapping results, reproduced in Fig. 3, showed that Co was concentrated at the extreme end of some of the larger Cu_6Sn_5 particles, consistent with a solidification catalyst effect.[14)]

The nucleation enhancement effect of Co also was supported by the calorimetric measurements, as indicated by the collection of heating and cooling thermograms of Fig. 4.[14)] The onset of the endothermic melting event for each alloy

Table 1 Asymmetric four point bend shear test results at ambient temperature from this study showing effect of solder joint aging as a percentage change in shear strength.

Alloy Designation	Nominal composition (mass%)				Shear ctrength @ 22°C (MPa)		Aging effect on shear strength (%)
	Sn	Ag	Cu	Co	As-cast	Aged	%Δ
Sn–Ag–Cu (NE)	Bal.	3.6	1.0	—	57, 57	50	−12
NE + 0.15Co	Bal.	3.6	1.0	0.15	46	40, 38	−15
NE + 0.45Co	Bal.	3.6	1.0	0.45	51, 51	51	0
Sn–3.5Ag	Bal.	3.5	—	—	53	42	−21

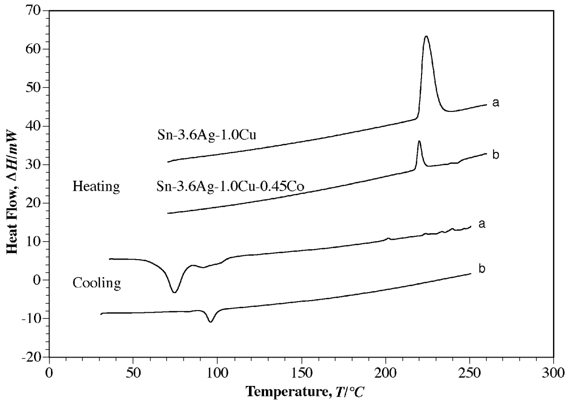

Fig. 4 Thermogram sections from differential scanning calorimetry measurements of the indicated alloys. Adapted from ref. 14).

(top two traces) occurs at about 217°C, essentially unaffected by the Co addition. The final melting event or liquidus temperature also appears similar. However, NE alloy droplets appear to solidify in about three different nucleation events, with smaller merged peaks at about 100°C and 90°C and a distinct major peak at about 75°C. In contrast, the NE + 0.45Co alloy droplets appear to solidify mainly within a singular peak at about 95°C, fully 20°C higher than the main peak of the NE alloy droplets. Such an enhanced nucleation temperature again would suggest the catalytic action of Co for the heterogeneous nucleation of solidification in this alloy system.

In addition to an apparent solidification catalyst effect that increased microstructural refinement, it was hypothesized[7,13] that Co also may promote microstructural stability and permit retained strength by modification of the coarsening behavior of a solder joint during high temperature aging. A summary of the AFPB shear strength measurements[14] that compare as-solidified solder joints to aged specimen behavior after exposure to 150°C for 72 hours is contained in Table 1, for the NE, NE + 0.15Co, NE + 0.45Co and Sn–3.5Ag alloy joints. Some replication of the measurements was performed, as indicated in Table 1, showing close agreement. SEM micrographs of equivalent as-solidified solder joints, prior to testing were provided in Fig. 2. As Table 1 shows, the Sn–3.5Ag joints exhibit a decrease of about 21% in maximum shear strength after aging. The NE alloy experiences a more moderate decrease (12%) in the maximum shear strength upon aging. The higher Co addition, 0.45Co, seems to suppress completely a reduction in strength from this level of aging.[14] However, the aging-induced strength reduction of the NE + 0.15Co solder joint appears very similar to the NE alloy. SEM analysis of the joint samples that were aged at 150°C is still in progress to identify the persistent microstructural characteristics of the Co-modified joint samples that promote strength retention.

4. Discussion

As an initial benefit for strengthening over the baseline Sn–Ag eutectic solder, the Sn–Ag–Cu near-eutectic alloy exhibits Cu_6Sn_5 primary phase particles dispersed in a ternary eutectic microstructure of highly refined intermetallic particles of both Ag_3Sn and Cu_6Sn_5. This near-eutectic joint microstructure is distinct from the coarse Sn dendrites with interdendritic eutectic (Sn + Ag_3Sn) of the Sn–Ag solder joint. The solder joints with the Co addition have a more complex, 3-phase morphology with additional strengthening from larger dispersed Cu_6Sn_5 phases. One reason for the complex microstructure of the Sn–Ag–Cu–Co alloys appears to be the solidification catalyst effect of Co that promotes reduced undercooling and seems to enhance the nucleation site density for the Cu_6Sn_5 phase. The occurrence of these effects is supported by evidence from both the calorimetry measurements of Fig. 4 and the Auger elemental mapping results of Fig. 3.[14] The substitution of a minor amount of Fe for Cu in a near-eutectic Sn–Ag–Cu solder also appeared to produce a catalytic effect and microstructural refinement in the results of some recent studies on solder joints made in a similar manner.[15] Additional measurements with these techniques, as well as high resolution microstructural studies are needed to more firmly establish these mechanisms and the generality of this type of catalytic action.

The influence of the solder joint interface and matrix microstructure characteristics should be reflected in the shear strength of the joints, assuming a high level of reproducibility of the results. Unfortunately, our experience[7] with the sensitivity of shear strength measurements to extrinsic variables, *e.g.*, joint porosity and joint gap, appears, at this point, to restrict our comparisons of shear strength to relative measurements within a set of AFPB bars that are cut from a single butt joint sample. With this limitation on the data in this report, relative comparisons of the heat treatment effects on the same alloy are more useful than absolute comparisons between alloys. Thus, the results from the limited set of data in Table 1 do indicate that a ranking of shear strength aging stability can be established with the NE + 0.45Co alloy most stable, the NE and the NE+0.15Co with moderately enhanced stability, and the Sn–3.5Ag alloy the least stable. Of course,

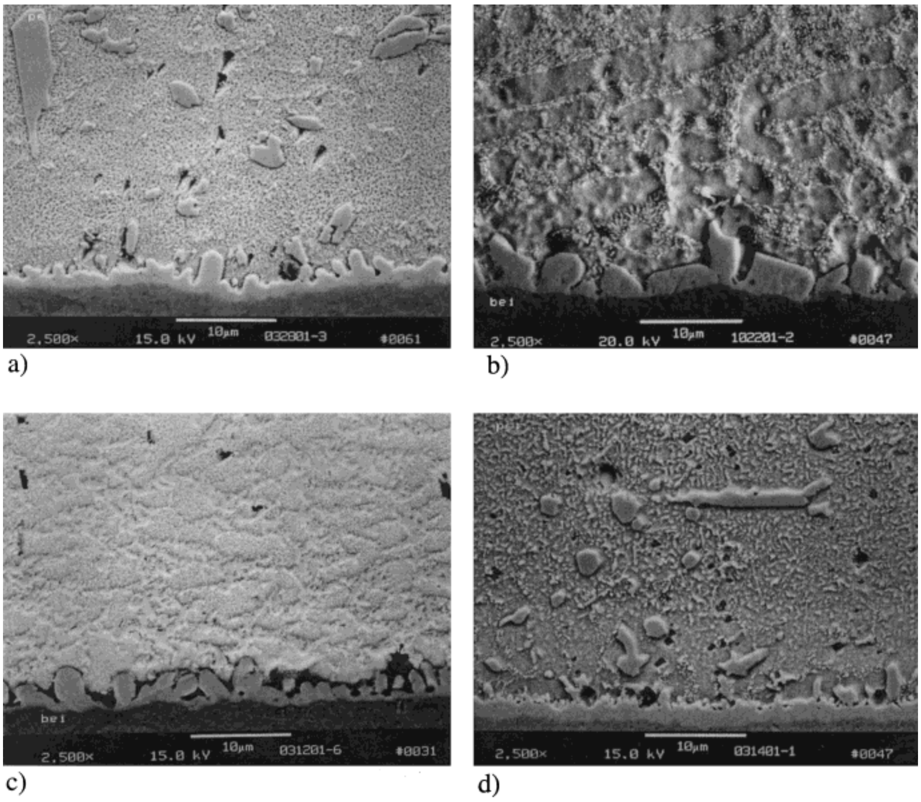

Fig. 5 SEM micrographs, using backscattered electron imaging, showing Cu substrate (bottom), intermetallic Cu/solder interface, and solder matrix microstructures at moderate magnification of slowly cooled joints made from a) Sn–3.6Ag–1.0Cu, b) Sn–3.7Ag–0.9Cu, c) Sn–3.6Ag–0.7Cu–0.2Fe, and d) Sn–3.7Ag–0.6Cu–0.3Co. Reprinted from ref. 16).

this ranking pertains to the specific sample preparation and test conditions, as well as the chosen aging temperature and duration.

As part of recent studies,[15,16] the soldering procedure was further refined to reduce porosity problems which promoted increased data reproducibility and permitted at least seven repeat tests for each condition. The major parameter changes were a reduction in the total flux addition and the restriction of flux application to only once, before heating. This procedure and the resulting mechanical properties are reported in detail, elsewhere.[15] In addition, an improvement of the previous quaternary alloying design was incorporated that involved a direct replacement of a portion of the Cu content in a Sn–3.7Ag–0.9Cu alloy by either Co or Fe. Following more closely a substitutional alloy design assumption,[13] this was accomplished by the direct substitution of either 0.3 mass%Co or 0.2 mass%Fe for the same mass%Cu in the alloys. This would limit the total content of “equivalent Cu” to be available for formation of Cu_6Sn_5 intermetallic in the as-solidified solder joint microstructure. Such a change was suggested by the results in this paper that showed an excess of blocky Cu_6Sn_5 phase in the solder matrix regions of Figs. 2(c) and (d). The excess Cu_6Sn_5 in the joint microstructure for additions of Co to Sn–3.6Ag–1.0Cu, was consistent with the Sn–Ag–Cu phase diagram assessment,[17] where the Cu_6Sn_5 phase certainly would be a primary solidification product.[15,16] Figure 5 shows the joint microstructures from the most recent study where the quaternary alloys contained less solute, resulting in less Cu_6Sn_5 primary phase.[15,16] Modification of the joint solidification microstructure in Fig. 5(b) by Fe or Co additions also is observed clearly in Figs. 5(c) and (d), respectively.[15,16]

To study the aging effects, more quantitative microstructural analysis is needed to characterize the differences in coarsening and diffusion processes that occur, along with some systematic variation of the aging parameters. A new study of aging will incorporate 100 h and 1,000 h aging at 150°C for the alloys in Fig. 5, along with Sn–3.0Ag–0.5Cu, Sn–3.9Ag–0.6Cu, and Sn–3.5Ag. Also, an extended series of thermal-mechanical fatigue studies are underway with some industrial partners to give an enhanced understanding of the reliability of solder joints made with this new family of Pb-free solders, beyond the encouraging shear strength results.

5. Summary

In this study, the microstructure and shear strength of Cu/solder/Cu solder joints made from Sn–Ag–Cu and Sn–Ag–Cu–Co alloys were characterized and compared to results for joints made from Sn–3.5Ag to provide a baseline. Shear strength was employed as a microstructure-sensitive mechanical property measurement to provide an indication of joint reliability. Microstructural analysis revealed that the Sn–Ag–Cu near-eutectic alloy exhibits a more highly refined microstructure containing intermetallic particles of both Ag_3Sn and Cu_6Sn_5, compared to the coarser Sn dendrite/eutectic structure of the Sn–Ag solder joint, containing Ag_3Sn intermetallics. The solder joints with the Co additions appear to have a more complex, 3-phase morphology with additional strengthening from larger dispersed Cu_6Sn_5 phases.

Calorimetry measurements and Auger elemental mapping results suggest that the microstructure of the Sn–Ag–Cu–Co alloys is influenced by a solidification catalyst effect from Co that promotes reduced undercooling and seems to enhance the nucleation site density for the Cu_6Sn_5 phase. Some recent additional results with Co and Fe additions are consistent with this catalysis effect, where a reduced total solute level was tested. Shear strength results indicate that a ranking of high temperature aging stability can be established with the $NE + 0.45Co$ alloy most stable, the NE and the $NE + 0.15Co$ with moderately enhanced stability, and the Sn–3.5Ag alloy the least stable.

Acknowledgements

Support for the fundamental aspects of this work is gratefully acknowledged from USDOE-BES, Materials Science Division under contract no. W-7405-Eng-82. Support for earlier applied aspects of this work is gratefully acknowledged from DOE-EM, under TTP no. CH133001, and, for recent applied work, from the Iowa State University Research Foundation, under grant no. 405-25-02. The Advanced Industrial Materials Program of the Office of Industrial Technologies of DOE-EE is also acknowledged for sponsoring a graduate student fellowship during an earlier stage of this study.

REFERENCES

1) I. E. Anderson, F. G. Yost, J. F. Smith, C. M. Miller and R. L. Terpstra: U.S. Patent No. 5,527,628, issued June 18, 1996.
2) C. M. Miller, I. E. Anderson and J. F. Smith: J. Electronic Materials **23** (1994) 595–601.
3) W. J. Plumbridge, C. R. Gagg and S. Peters: J. Electronic Materials **30** (2001) 1178–1183.
4) J. Bath, C. Handwerker and E. Bradley: Circuits Assembly (May 2000) pp. 31–40.
5) Challenges and Efforts Toward Commercialization of Lead-free Solder-Road Map 2000 for Commercialization of Lead-free Solder-ver 1.2, The Japan Electronic Industry Development Association, Lead-free Soldering R&D Project Committee, February 2000; http://www.jeida.or.jp/english/information/pbfree/roadmap.html.
6) I. E. Anderson, O. Unal, T. E. Bloomer and J. C. Foley: *The Third Pacific Rim International Conference on Advanced Materials and Processing*, (The Minerals, Metals and Materials Society, 1998) **2**, p. 189.
7) I. E. Anderson, T. E. Bloomer, R. L. Terpstra, J. C. Foley, B. A. Cook and J. L. Harringa: *Advanced Brazing and Soldering Technologies*, ed. by P. T. Vianco and M. Singh (American Welding Society, 2000) pp. 575–586.
8) I. E. Anderson, T. E. Bloomer, J. C. Foley and R. L. Terpstra: IPC Works '99, (IPC, Northbrook, IL, 1999) paper No. S-03-5.
9) M. McCormack and S. Jin: J. of Minerals, Metals and Materials (1993) pp. 36–40.
10) O. Unal, I. E. Anderson, J. L. Harringa, R. L. Terpstra, B. A. Cook and J. C. Foley: J. Electronic Materials **30** (2001) 1206–1213.
11) C. M. Liu, C. E. Ho, W. T. Chen and C. R. Kao: J. Electronic Materials **30** (2001) 1152–1156.
12) I. E. Anderson and J. H. Perepezko: *Grain Refinement in Castings and Welds*, ed. by G. J. Abbaschian and S. A. David (The Metallurgical Society of AIME, 1983) pp. 67–86.
13) I. E. Anderson and R. L. Terpstra: U.S. Patent No. 6,231,691 B1, issued May 15, 2001.
14) I. E. Anderson, J. C. Foley, B. A. Cook, J. L. Harringa, R. L. Terpstra and O. Unal: J. Electronic Materials **30** (2001) 1050–1059.
15) I. E. Anderson, B. A. Cook, J. Harringa and R. L. Terpstra: accepted for publication in J. Electronic Materials (2002).
16) I. E. Anderson, B. A. Cook, J. L. Harringa and R. L. Terpstra: J. of Minerals, Metals and Materials **54** (2002) 26–29.
17) K.-W. Moon, W. J. Boettinger, U. R. Kattner, F. S. Biancaniello and C. A. Handwerker: J. Electronic Materials **29** (2000) 1122–1136.